Thermal Analysis of Modular Multilevel Converters Under Subsynchronous Oscillation

Yongxia Liu, Jing Sheng, Yufei Dong, Renju Zheng, Wuhua Li, Xiangning He, Zhichao Zhou
College of Electrical Engineering ,Zhejiang University
Hangzhou, China
Email:woohualee@zju.edu.cn

Rui Xie
Zhejiang Electric Power Design Institute of China Energy Engineering Group
Hangzhou, China
Email: zrxd@sina.com

***Abstract*—Subsynchronous oscillation (SSO) may occur in modular multilevel converter based high-voltage direct-current (MMC-HVDC) system, leading to overcurrent and overheating of power devices in MMCs, thus threatening the reliability of MMCs. As the mechanism of SSO in MMC-HVDC has not been clarified, it is essential to investigate the thermal performance of power devices to promote the reliability of MMCs. In this paper, junction temperature is calculated by the power loss model and thermal network. Then, the relationship between junction temperature and SSO frequency is investigated. It is concluded that with the increase of SSO frequency, both the maximum junction temperature and thermal cycling go down firstly and then go high, and both are lowest when SSO frequency is 25Hz. Further investigation reveals that the low frequency loss fluctuation caused by SSO is the main cause to this thermal phenomenon. Finally, a simulation model and an MMC prototype with six sub-modules per arm are established to verify the theoretical analysis.**

Keywords—subsynchronous oscillation, modular multilevel converter, thermal analysis

I. INTRODUCTION

Voltage sourced converters based high-voltage direct-current (VSC-HVDC) system has received increasing attention as a practicable scheme for efficient renewable energy integration over long distances [1-3]. Modular multilevel converter based high voltage direct current (MMC-HVDC) transmission technology is considered as one of the promising solutions for grid integration of large and remote offshore wind farms due to its lower harmonic components, high conversion efficiency and lower manufacturing difficulty [4-5].

It is reported that the subsynchronous oscillation (SSO) phenomenon may occur in MMC-HVDC system for wind farm integration [6]. With subsynchronous oscillation current added, operating current goes higher, leading to the overcurrent issue of MMC and overheating issue in power devices. Since power devices are critical components for the reliability of MMC and thermal stress is the main reason responsible for the failure of power devices, thermal performance of power devices is significant for the reliability of MMC [7-10]. With increased power rating of MMC and increased output current requirement, if MMC-HVDC system cannot withstand SSO, failure or shutdown of MMC may cause serious problem. In consequence, in order to enhance the reliability of MMC, it is essential to analyze the impacts of SSO on MMCs, especially the thermal performance of power devices of MMCs.

The impacts of SSO on MMCs' loading profile is investigated in [6,11], where the impedance characteristics of system are discussed, but the mechanism of SSO is not clarified. In addition, impedance-based analytical approach is applied to analyzed the stability of MMC-HVDC under SSO through the Nyquist diagrams in frequency domain in [6], which reveals that SSO is caused due to interactions between the MMC and the wind power inverters. However, the explicit origin of SSO is not mentioned. A small-signal dynamic dq model of MMC is established in [12], but this model, which consists of different dq rotating frames, is too complicated to provide useful information concerning the causes of SSO. Therefore, considering that the mechanism of SSO of MMCs in MMC-HVDC transmission system is still not revealed, the thermal behavior of MMC is supposed to be comprehensively investigated to avoid the breakdown of MMC under SSO.

In contrast to the conventional converters, topology and control methods of MMCs make their thermal performance different. When SSO occurs, with currents and junction temperatures go high, thermal performance of power devices is the key factor for the reliability of converter. In [13-15], The thermal distribution of MMC for motor drivers, smart transformers and wind power transmission applications are investigated respectively. Besides, the overload capacity of MMC in terms of thermal behaviors of power devices is exploited in [16] and thermal cycling of MMC for offshore wind power is discussed in [17]. Reference [18] provides thermal analysis of the MMC in operation at low power factor. Although there are many literatures analyzing the thermal performance of MMC, thermal behaviors of power devices of MMC have not been investigated in MMC-HVDC system under SSO.

This paper aims to explore the impact of subsynchronous oscillation frequency on thermal performance of power devices in MMC-HVDC systems. In Section II, the system configuration is introduced, and then, the method to calculate the power loss of power devices and thermal network are shown. In Section III, power loss of power devices is expressed clearly. Thus, thermal performance of power devices are analyzed and the relationships between SSO frequency and junction temperature become clear. The analytical results are verified by simulation and MMC prototype in Section IV. Finally, the conclusions are given in Section V.

This work is sponsored by the National Key Research and Development Program of China (2017YFE0112400) and the National Nature Science Foundations of China (51490682, 51677166).

II. System Configuration and Thermal Model of MMC Under SSO

A. System Configuration

A typical circuit configuration of MMC-HVDC system for wind farm integration is shown in Fig.1, where the sending-end converter (SEC) is implemented by MMC rectifier. Star-delta transformers *T1* are employed to block the zero-sequence path between the power system and MMC. The circuit structure of half-bridge based MMC is shown in Fig.2, where each phase has two arms and each arm consists of one arm inductor L_{Arm} and N identical half-bridge sub-modules (SMs).

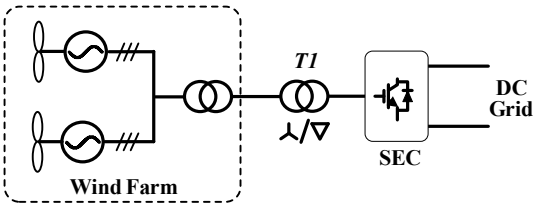

Fig.1 Circuit configuration of MMC-HVDC system.

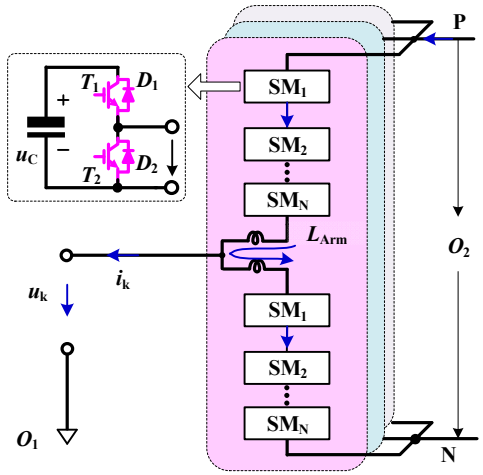

Fig.2 Circuit structure of half-bridge based MMC.

B. Thermal Model of MMC Under SSO

SSO currents of three phases added to AC side of MMC can be expressed as follows [11].

$$\begin{cases} i_{a\_ss}(t) = I_{m\_ss}\sin(\omega_{ss}t) \\ i_{b\_ss}(t) = I_{m\_ss}\sin(\omega_{ss}t - \dfrac{2\pi}{3}) \\ i_{c\_ss}(t) = I_{m\_ss}\sin(\omega_{ss}t + \dfrac{2\pi}{3}) \end{cases} \tag{1}$$

where $i_{a\_ss}(t)$, $i_{b\_ss}(t)$ and $i_{c\_ss}(t)$ denote SSO currents of phase *a*, *b* and *c*, respectively, I_{m_ss} is amplitude of SSO current, ω_{ss} represents the frequency of SSO.

Take phase *a* as an example. Assuming that circulating current has been suppressed, the upper and lower arm currents, $i_{ap}(t)$ and $i_{an}(t)$, can be expressed as (2) under SSO.

$$\begin{cases} i_{ap}(t) = \dfrac{I_{dc}}{3} + \dfrac{1}{2}I_m\sin(\omega t) + \dfrac{1}{2}I_{m\_ss}\sin(\omega_{ss}t) \\ i_{an}(t) = \dfrac{I_{dc}}{3} - \dfrac{1}{2}I_m\sin(\omega t) - \dfrac{1}{2}I_{m\_ss}\sin(\omega_{ss}t) \end{cases} \tag{2}$$

where I_{dc} is DC output current, ω is rated frequency, and I_{m} is the amplitude of rated current. As AC voltages of MMC are not affected by SSO [11], the upper and lower arm voltages, $u_{\mathrm{ap}}(t)$ and $u_{\mathrm{an}}(t)$, can be written as

$$\begin{cases} u_{ap}(t) = \dfrac{U_{dc}}{2} - U_m\sin(\omega t + \varphi) \\ u_{an}(t) = \dfrac{U_{dc}}{2} + U_m\sin(\omega t + \varphi) \end{cases} \tag{3}$$

where U_{dc} is DC output voltage, U_{m} is the amplitude of AC output voltage, and φ is the phase displacement between power voltage and power current.

To obtain thermal performances of power devices of MMC, loss of power devices should be figured out under SSO. Taking IGBT T_1 for example, power losses consist of conduction loss and switching loss. T_1 of upper arm SMs don't work when $i_{\mathrm{ap}}(t)\geqslant 0$. So when $i_{\mathrm{ap}}(t)<0$, conduction loss and switching loss of T_1, $p_{\mathrm{Con\_T1}}(t)$ and $p_{\mathrm{Swt\_T1}}(t)$, can be expressed as (4) and (5), respectively.

$$p_{Con\_T1}(t) = -i_{ap}(t)\cdot V_{Con\_T}\cdot d_{S1}(t) \tag{4}$$

$$\begin{aligned} p_{Swt\_T1}(t) &= E_{Sw\_T}(-i_{ap}(t))\cdot f_{sw} \\ &= \left\{A_T\cdot\left[-i_{ap}(t)\right]^2 + B_T\cdot\left[-i_{ap}(t)\right] + C_T\right\}\cdot f_{sw} \end{aligned} \tag{5}$$

where $V_{\mathrm{Con\_T}}$ denotes the on-state voltage drop, $d_{\mathrm{S1}}(t)$ is the duty cycle of S_1, f_{sw} is switching frequency when $i_{\mathrm{ap}}(t)<0$, and $E_{\mathrm{Sw\_T}}(i(t))$, the switching loss energy at the instant when the commutation current is $i(t)$, can be fitted by quadratic polynomial with the coefficient A_{T}, B_{T} and C_{T} from the test curve shown in the datasheet.

Junction temperatures of power devices can be obtained by the thermal network indicated in Fig.3 after the power losses are calculated. In the four-layer Foster *RC* thermal network, the current at the point A in the Foster thermal network is the power loss, and then the voltage at the point A is the junction temperature. Thus, junction temperatures of power devices is mainly determined by their power losses.

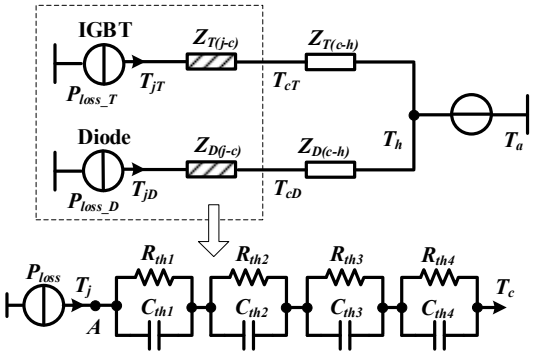

Fig.3 Thermal network of a power semiconductor device.

III. Thermal Performance Analysis of MMC Under SSO

Taking diode D_2 in a SM of phase a for example, diode D_2 is off when $i_{ap}(t) \geqslant 0$, that is, $p_{loss\_D2}(t) = 0$. From (2) - (5), when $i_{ap}(t) < 0$, power losses of D_2 can be expressed as

$$\begin{aligned} p_{loss\_D2}(t) = {} & k_1 + k_2 \sin(\omega t + \varphi_1) + k_3 \sin(\omega_{ss} t) \\ & + k_4 \sin(2\omega t + \varphi_2) + k_5 \cos(2\omega_{ss} t) \\ & + k_6 \sin[(\omega + \omega_{ss})t + \varphi_3] \\ & + k_7 \sin[(\omega - \omega_{ss})t + \varphi_4] \end{aligned} \tag{6}$$

where k_i and φ_j (i=1~7, j=1~4) are determined by I_{dc}, I_m, I_{m_ss}, f_{sw}, m, φ, V_{Con_x}, A_x, B_x, C_x (x=T or D).

From (6), power losses of power devices consist of DC component and frequency components of ω, ω_{ss}, 2ω, $2\omega_{ss}$, $\omega+\omega_{ss}$ and $\omega-\omega_{ss}$. Therefore, thermal distribution of MMC is influenced by these various frequency components of power losses.

Since the expressions of k_i and φ_j (i=1~7, j=1~4) are complicated, a case can help demonstrate the meaning of (6) with parameters in Table I.

TABLE I. Critical Parameters for Analysis and Simulation

Items	Values
Rated active power P	20MW
Peak value of DC voltage U_{dc}	20kV
Peak value of AC voltage U_m	15kV
Switching frequency f_{sw}	150Hz
Rated frequency f	50Hz
Ambient temperature T_h	60 ℃
I_{m_ss} / I_m	0.5
Modulation ratio m	0.8
IGBT Module (ABB)	5SNA1200E330100

From the thermal network shown in Fig.3 and the expression of power loss of D_2 in (6), the junction temperature of D_2 can be calculated. As an example, the waveform of junction temperature of D_2 is shown in Fig.4 with SSO frequency of 2.5Hz. From Fig.4, the maximum junction temperature of D_2 is 107 ℃ and the thermal cycling value is 20 ℃.

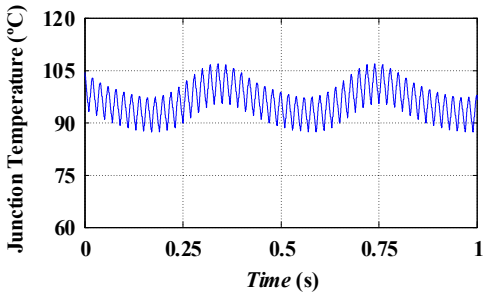

Fig.4 The waveform of junction temperature of D_2 with SSO frequency of 2.5Hz.

Fig.5 illustrates the maximum junction temperatures and thermal cycling values of D_2 with various SSO frequencies. Both the maximum junction temperature and thermal cycling go down firstly and then go high, and both are lowest when SSO frequency is 25Hz. From the thermal network shown in Fig.3, thermal impedance from junction to case $Z_{T(j\text{-}c)}$ and $Z_{D(j\text{-}c)}$ is modeled with four-layer Foster RC network, and thermal impedance from case to heat sink $Z_{T(c\text{-}h)}$ and $Z_{D(c\text{-}h)}$ is modeled with a thermal resistance. It means that junction temperature of power device goes high with the decrease of frequency of loss because of the capacitors C_{th1}~C_{th4}. This has been shown in Fig.5 that the low frequency component of power losses contributes prominent rise to the junction temperature. In addition, the lower the frequency of power loss is, the more this frequency component of power loss contributes to junction temperature. For example, as is shown is Fig.4, f_{ss} (2.5Hz) is the minimum frequency of power loss components, so $k_3\sin(\omega_{ss}t)$ contributes prominent rise to the junction temperature.

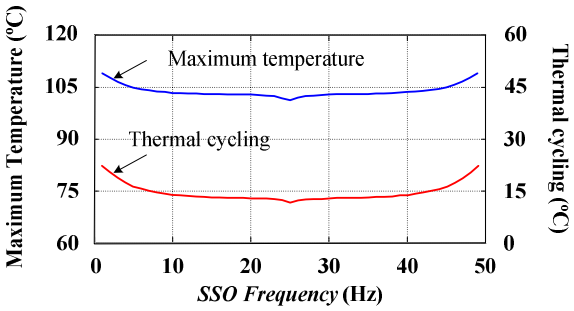

Fig.5 The maximum junction temperature and thermal cycling of D_2 with various SSO frequencies.

IV. Simulation and Experimental Verification

A. Simulation

A three-phase MMC MATLAB/Simulink system is established with the parameters in Table I and N=10 SMs per arm.

Junction temperatures of 4 power devices in an SM is shown in Fig.6 a) - d), which compares the junction temperature waveforms of normal operation with that of SSO frequency f_{ss} = $\omega_{ss}/(2\pi)$ = 2.5Hz, 10Hz, 25Hz and 47.5Hz, respectively. From Fig.6 a) - d), it is obvious that the maximums and thermal cycling values of junction temperatures under SSO are higher than that without SSO, and that junction temperature of diode D_2 is highest among 4 power devices. Moreover, with the SSO frequency of 2.5Hz, 10Hz, 25Hz and 47.5Hz, the maximum junction temperatures are 113.31 ℃, 107.35 ℃, 101.06 ℃ and 105.87 ℃, respectively, and the thermal cycling values are 34.51 ℃, 24.55 ℃, 16.70 ℃ and 24.97 ℃, respectively.

Taking D_2 for example, as is illustrated in Fig.6 and Fig.7, the maximum of junction temperature T_{jD2} goes down firstly and then goes high with the increase of SSO frequency f_{ss}. Also, the thermal cycling values of D_2 goes down firstly and then goes high with the increase of f_{ss}. This phenomenon can be explained by the theoretical analysis in Section III. In Fig.6 a), when f_{ss} is little (e.g. 2.5Hz), f_{ss} is the minimum frequency of power loss components, so $k_3\sin(\omega_{ss}t)$ contributes prominent rise to the junction temperature.

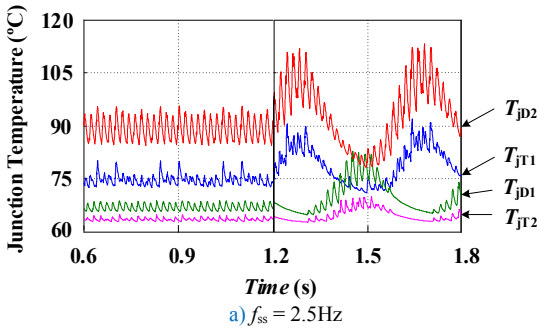

a) f_{ss} = 2.5Hz

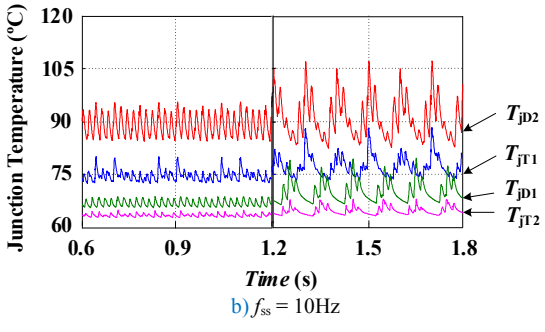

b) f_{ss} = 10Hz

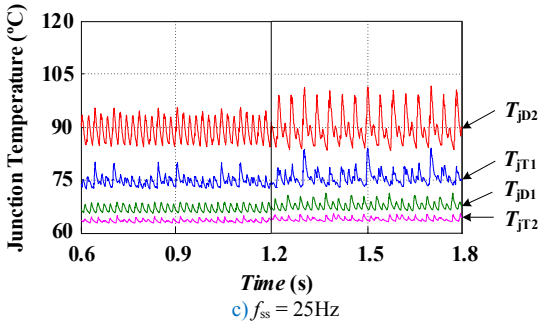

c) f_{ss} = 25Hz

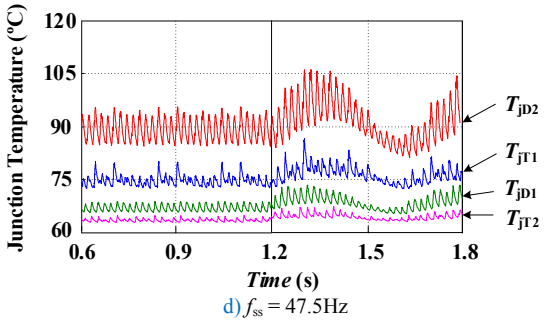

d) f_{ss} = 47.5Hz

Fig.6 Waveforms of power devices' junction temperatures in an SM.

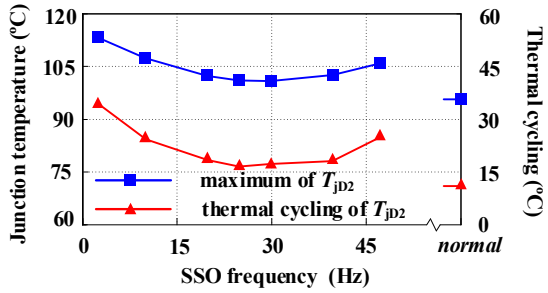

Fig.7 Relationship between T_{jD2} and f_{ss}.

Similarly, in Fig.6 c), when f_{ss} is 25Hz, there is not a very small frequency among frequency components of power losses, and thus maximum junction temperature is lower. Moreover, in Fig.6 d), when f_{ss} is slightly less than 50Hz (e.g. 47.5Hz), f - f_{ss} is the minimum frequency of loss components, so $k_7\sin[(\omega-\omega_{ss})t+\varphi_4]$ contributes prominent rise to the junction temperature.

In conclusion, the theoretical analysis has been verified that with the increase of SSO frequency, both the maximum junction temperature and thermal cycling go down firstly and then go high, and both are lowest when SSO frequency is 25Hz. Also, the prominent contribution of low frequency loss fluctuation to devices' thermal performance is explained.

B. *Experimental Verification*

Verification of the analysis is implemented in a scaled-down MMC prototype. The specifications and critical parameters of the tested MMC are given in Table II. The MMC is connected to an AC programmable source and operates as a rectifier. As the cause of SSO is unknown, it is difficult to reproduce it. Thus, in this test, subsynchronous oscillation is added to the AC side of MMC artificially. In the test, the MMC is modulated with the phase-shift PWM and the circulating current has been suppressed. As diode D_2 has the highest junction temperature among 4 power devices, only the temperature of D_2 is tested. And the AC source and the MMC are not recommended to operate at very low frequency, so 15Hz, 25Hz and 35Hz are chosen as the tested SSO frequencies.

TABLE II. EXPERIMENTAL PARAMETERS OF MMC TEST BENCH

Items	Values
Rated active power P	4kW
Rated DC grid voltage U_{dc}	400V
Rated MMC AC voltage U_m	113V
Sub-module capacitor voltage U_C	100V
Sub-module capacitance C_{sm}	4.8mF
Rated frequency f	50Hz
Ambient temperature T_h	60 ºC
I_{m_ss} / I_m	0.3

In Fig.8, When MMC operates normally, the waveform of temperature of D_2 is stable. It must be mentioned that the waveform is stable compare to Fig.6 in simulation because of the air cooling system. In simulation, it is assumed that the temperature of heat sink is constant, so the capacitance of the thermal network is less than that in the experiment. Thus, the waveform of temperature is more stable in the experiment.

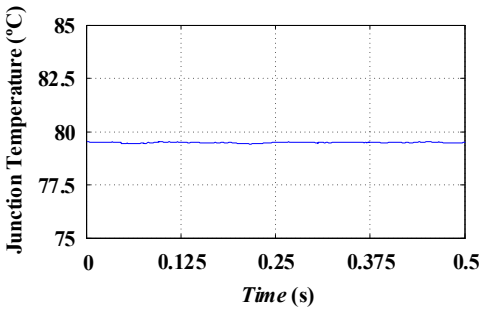

Fig. 8 Waveforms of temperature of D_2 when MMC operates normally.

When MMC operate with the SSO frequency of 35Hz, the waveforms and thermal performance are shown in Fig.9. Fig.9 a) illustrates the voltage and currents of arm and AC current of phase *a*. It is obvious that AC current of phase *a* added 35Hz SSO current on rated frequency 50Hz. In Fig.8 b), the waveform of temperature of D_2 contains fluctuation of 15Hz caused by the 15Hz component of power losses because the difference of 50Hz and 35Hz (that is, 15Hz) is the lowest frequency of power devices and 15Hz component of power losses contributes prominent rise to the temperature of D_2.

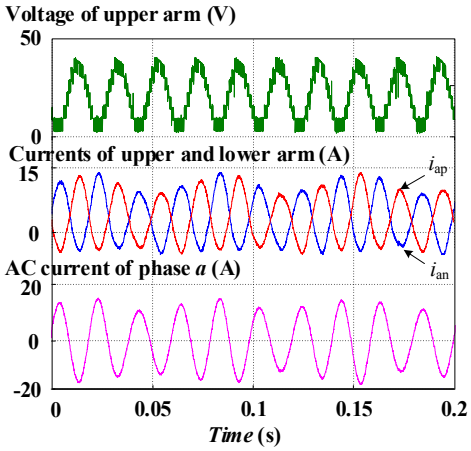

a) waveforms of voltage and currents of arms and AC side

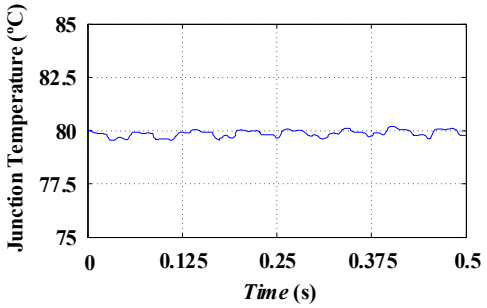

b) waveform of temperature of D_2

Fig.9 Waveforms when f_{ss} = 35Hz.

Fig.10 shows the temperature performance of D_2 when MMC operates when f_{ss} = 25Hz and 15Hz. In Fig.10 a), SSO frequency is 25Hz. It is obvious that the waveform of temperature of D_2 contains the 25Hz component, caused by the 25Hz components of power losses. And similarly, in Fig.9 b), when SSO frequency is 15Hz, 15Hz component of temperature is distinct.

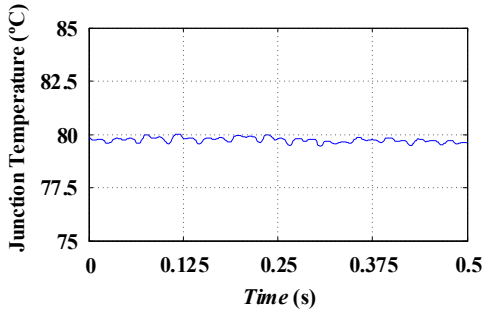

a) f_{ss} = 25Hz

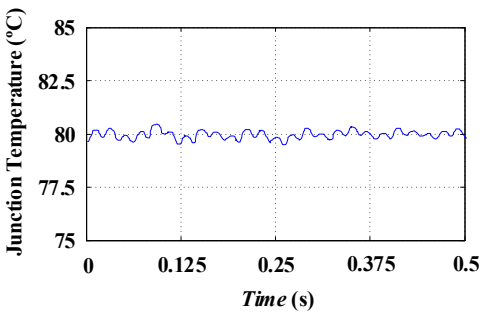

b) f_{ss} = 15Hz

Fig.10 Waveforms of temperature of D_2 when f_{ss} = 25Hz and f_{ss} = 15Hz.

In Fig.8, the maximum temperature of D_2 is 79.55 ºC and the thermal cycling value is 0.21 ºC. In Fig.9 and Fig.10, the maximum temperature of D_2 is 80.48 ºC, 80.03 ºC and 80.34 ºC and the thermal cycling value is 1.03 ºC, 0.55 ºC and 0.80 ºC, respectively, when the SSO frequency is 15Hz, 25Hz and 35Hz, respectively. Thus, it can be verified that with the increase of SSO frequency, both the maximum junction temperature and thermal cycling values go down firstly and then go high, and both are lowest when SSO frequency is 25Hz.

V. CONCLUSIONS

In conclusion, SSO does lead to the rise of maximum and average junction temperatures of power devices of MMC in MMC-HVDC transmission system. Theoretical thermal analysis leads to the conclusion that with the increase of SSO frequency, both the maximum junction temperature and thermal cycling values go down firstly and then go high, and both are lowest when SSO frequency is 25Hz. It is revealed that the low frequency loss fluctuation caused by SSO is the main cause to this thermal phenomenon. Finally, the simulation and experimental results have verified the theoretical analysis.

REFERENCES

[1] Bresesti P, Kling W L, Hendriks R L, et al. HVDC connection of offshore wind farms to the transmission system[J]. Energy Conversion, IEEE Transactions on, 2007, 22(1): 37-43.

[2] Flourentzou N, Agelidis V G, Demetriades G D. VSC-based HVDC power transmission systems: An overview[J]. Power Electronics, IEEE Transactions on, 2009, 24(3): 592-602.

[3] Ahmed N, Haider A, Van Hertem D, et al. Prospects and challenges of future HVDC SuperGrids with modular multilevel converters[C]//Power Electronics and Applications (EPE 2011), Proceedings of the 2011-14th European Conference on. IEEE, 2011: 1-10.

[4] C. Du, M. H. J. Bollen, E. Agneholm and A. Sannino, "A new control strategy of a VSC–HVDC system for high-quality supply of industrial plants," IEEE Trans. Power Del., vol. 22, no. 4, pp. 2386-2394, Oct. 2007.

[5] K. Friedrich, "Modern HVDC PLUS application of VSC in modular multilevel converter topology," Proc. IEEE Int. Symp. Ind. Electron., pp. 3807-3810, Nov. 2010.

[6] Jing Lyu, Xu Cai and Marta Molinas, "Frequency domain stability analysis of MMC-based HVDC for wind farm integration," IEEE Journal of Emerging & Selected Topics in Power Electronics, vol. 4, no. 1, pp. 141-151, Mar. 2016.

[7] S. Yang, D. Xiang, A. Bryant, P. Mawby, L. Ran, P. Tavner, "Condition monitoring for device reliability in power electronic converters: A review," *IEEE Trans. Power Electron.*, vol. 25, no. 11, pp. 2734-2752, Nov. 2010.

[8] D. Hirschmann, D. Tissen, S. Schroder, R. W. De Doncker, "Reliability prediction for inverters in hybrid electrical vehicles," *IEEE Trans. Power Electron.*, vol. 22, pp. 2511-2517, Nov. 2007.

[9] A. Bryant, N. A. Parker-Allotey, P. Palmer, "The use of condition maps in the design and testing of power electronic circuits and devices," *IEEE Trans. Ind. Appl.*, vol. 43, no. 4, pp. 874-883, Jul. 2007.

[10] D. Zhou, F. Blaabjerg, T. Franke, M. Tonnes, M. Lau, "Optimized reactive power flow of DFIG power converters for better reliability performance considering grid codes," *IEEE Trans. Ind. Electron.*, vol. 62, no. 3, pp. 1552-1562, Mar. 2015.

[11] Jing Lv, Peng Dong, Gang Shi, Xu Cai and Xiaolin Li, "Subsynchronous oscillation and its mitigation of MMC-based HVDC with large doubly-fed induction generator-based wind farm integration," Proceedings of the CSEE, vol.35, no. 19, pp. 4852-4860, Oct. 2015.

[12] Jamshidifar A and Jovcic D, "Small-signal dynamic DQ model of modular multilevel converter for system studies," IEEE Transactions on Power Delivery, vol. 31, no. 1, pp. 191-199, May. 2015.

[13] S. Rohner, S. Bernet, M. Hiller and R. Sommer, "Modulation losses and semiconductor requirements of modular multilevel converters," IEEE Trans. Ind. Electron., vol. 57, no. 8, pp. 2633-2642, Aug. 2010.

[14] M. Andresen, K. Ma, G. D. Carne, G. Buticchi, F. Blaabjerg and M. Liserre, "Thermal Stress Analysis of Medium Voltage Converters for Smart Transformers," IEEE Trans. Power Electron., vol. 32, no. 6, pp. 4753- 4765, Jun. 2017

[15] X. Han, Q. Yang, L. Wu and M. Saeedifard, "Analysis of thermal cycling stress on semiconductor devices of the Modular Multilevel Converter for drive applications," in Proc. IEEE Appl. Power Electron. Conf. Expo., pp. 2957-2962, May 2016.

[16] Paul D. Judge and Timothy C. Green. "Dynamic thermal rating of a modular multilevel converter HVDC link with overload capacity," PowerTech, 2015 IEEE Eindhoven. IEEE, 2015, pp. 1-6.

[17] H. Liu, K. Ma, Z. Qin, P. C. Loh and F. Blaabjerg, "Lifetime Estimation of MMC for Offshore Wind Power HVDC Application," IEEE J. Emerg. Sel. Topics Power Electron., vol. 4, no. 2, pp. 504-511, June 2016.

[18] F. Hahn, M. Andresen, G. Buticchi and M. Liserre. "Thermal Analysis and Balancing for Modular Multilevel Converters in HVDC Applications," IEEE Trans. Power Electron., vol. 33, no. 3, pp. 1985-1996, Apr. 2017.